Biophysical Chemistry 147 (2010) 20–27

Contents lists available at ScienceDirect

Biophysical Chemistry

journal homepage: http://www.elsevier.com/locate/biophyschem

Properties of phosphatidylcholine in the presence of its monofluorinated analogue

Eric A. Smith, Christiaan M. van Gorkum, Phoebe K. Dea *

Department of Chemistry, Occidental College, 1600 Campus Road, Los Angeles, CA 90041, USA

ARTICLE INFO

Article history:
Received 31 October 2009
Received in revised form 15 December 2009
Accepted 15 December 2009
Available online 24 December 2009

Keywords:
Fluorinated phospholipid
Interdigitated phase
Differential scanning calorimetry
DPH fluorescence
Phase separation
Domain formation

ABSTRACT

In aqueous solution, the monofluorinated phospholipid 1-palmitoyl-2-[16-fluoropalmitoyl]sn-glycero-3-phosphocholine (F-DPPC) interdigitates without the use of inducing agents. To understand the thermal and physical properties of this unique lipid, F-DPPC was combined with the non-fluorinated 1,2-dipalmitoyl-*sn*-glycero-3-phosphocholine (DPPC), and 1,2-diarachidoyl-*sn*-glycero-3-phosphocholine (DAPC). Differential scanning calorimetry (DSC) was used to determine the miscibility and thermotropic phase behavior of these binary lipid mixtures. In addition, the fluorescent probe 1,6-diphenyl-1,3,5-hexatriene (DPH) and a DPH-labeled analogue of DPPC, 2-(3-(diphenylhexatrienyl) propanoyl)-1-hexadecanoyl-*sn*-glycero-3-phosphocholine (β-DPH HPC, aka DPH-PC or DPHpPC), were used to detect interdigitation. In F-DPPC, the fluorescence intensity of both probes decreased a similar amount and to a degree that is consistent with an interdigitated system. We also determined that there are two separate effects of increasing the ratio of F-DPPC in the DPPC/F-DPPC system. With low amounts of F-DPPC, there is little evidence that the system is heavily interdigitated. Instead, we hypothesize that the introduction of F-DPPC provides nucleation sites that alter the kinetics, reversibility, and temperature of the main transition (T_m). At higher mol% of F-DPPC, we propose that interdigitated F-DPPC-rich domains form to create a phase-segregated system. While DPPC/F-DPPC was highly miscible, the DAPC/F-DPPC system was significantly less miscible. Additionally, we observed that DAPC/F-DPPC samples have reduced solubility in water, which affected the acquisition of fluorescence data. However, our DSC results indicate the existence of DAPC-rich and F-DPPC-rich components. Furthermore, this data support that the mixing was disruptive to lipid packing and that the presence of DAPC hinders the interdigitation of F-DPPC.

1. Introduction

The interdigitated gel phase ($L_{\beta}I$) is a unique bilayer conformation in which the hydrocarbon chains of the lipids interpenetrate into the opposing monolayer. These systems can thereby maximize Van der Waals forces and reduce headgroup crowding [1–3]. Under normal circumstances, the interdigitated phase is not energetically favored in lipids like DPPC and DAPC because the hydrophobic tails are exposed to the aqueous medium. However, in the presence of inducer molecules such as short chain alcohols and some anesthetics, the hydrocarbon-aqueous tension is reduced so that interdigitation can occur [3–5]. The application of pressure can also induce interdigitation [6,7].

Therefore, it is of great interest to study lipids that automatically form partially-, mixed-, or fully-interdigitated bilayers in aqueous solution without inducer chemicals or external pressure. Of these lipids, F-DPPC is distinct because it differs from DPPC only by a single fluorine atom substitution. Other lipids are known to self-assemble into the interdigitated state, but are usually highly asymmetrical lipids such as lysolipids or lipids with acyl chains of two different lengths (for review see [1]).

Hirsh et al. were the first to find that the monofluorinated F-DPPC fully interdigitates on its own [8]. They attributed this behavior to the highly polar fluorine bond at the end of one of the hydrocarbon chains, which makes the terminal end more hydrophilic. Hirsh et al. also determined that the main transition temperature (T_m) of F-DPPC to be ~50 °C in aqueous solution. Therefore, we chose DAPC and DPPC for our binary mixtures with F-DPPC because their T_m phase transition temperatures are above and below that of F-DPPC respectively. All three lipids share the same headgroup and have fully saturated acyl chains as well. Based on previous experiments, we hypothesized that the lipids would be at least partially miscible [9,10].

Due to their versatility, fluorinated lipids are prime candidates for artificial membrane research and as membrane probes. For instance, the fluorine-modified acyl chains can enhance the hydrophobic and lipophobic interactions that control the T_m and the solubility of lipophilic probes [11]. Furthermore, these modifications alter membrane fluidity and structure [12], permeability [13], and the behavior of

Abbreviations: DSC, differential scanning calorimeter; T_m, main transition temperature; L'_{β}, planar gel phase; P'_{β}, ripple gel phase; L_{α}, liquid crystalline phase; $L_{\beta}I$, interdigitated gel phase, DPPC, 1,2-dipalmitoyl-*sn*-glycero-3-phosphocholine; F-DPPC, 1-palmitoyl-2-[16-fluoropalmitoyl]-sn-glycero-3-phosphocholine; DAPC, 1,2-diarachidoyl-*sn*-glycero-3-phosphocholine; DPH, 1,6-diphenyl-1,3,5-hexatriene; β-DPH HPC, 2-(3-(diphenylhexatrienyl) propanoyl)-1-hexadecanoyl-*sn*-glycero-3-phosphocholine.

* Corresponding author. Tel.: +1 323 259 2625; fax: +1 323 341 4912.
E-mail address: dea@oxy.edu (P.K. Dea).

0301-4622/$ – see front matter © 2009 Elsevier B.V. All rights reserved.
doi:10.1016/j.bpc.2009.12.005

lipids in biological media [14]. Additionally, fluorine-labeled phospholipids can be used to study the properties of membrane proteins with ^{19}F NMR [15]. They can also be used as potential vehicles for drug delivery, such as thermosensitive liposomes that can regulate medicine release [16].

DSC experiments by Rolland et al. [17] have shown that the miscibility of highly fluorinated glycerophosphocholines when combined with the unmodified parent lipids depends on the location and number of fluorine substitutions. This is important because the miscibility between liposome and cellular lipids controls membrane fusion, interactions with lipoproteins, and the effectiveness of drug delivery [17]. Also, Sturtevant et al. found that various difluorinated phospholipids have greater transition enthalpies and form nonideal mixtures with the parent compounds [18]. For these reasons, we set out to determine how the monofluorinated F-DPPC behaves when combined with naturally occurring lipids.

Furthermore, since F-DPPC interdigitates, it can provide information on lipid domains and phase behavior. Previous experiments have explored domain formation and phase separation in lipid mixtures involving different chain lengths [19–21], headgroups [22], the presence of cholesterol [23], and degrees of unsaturation [24]. In particular, work by Rowe [25] and Mason [26] has shown that it is possible to have coexisting gel and interdigitated phases. Rowe demonstrated that a mixture of dilaurylphosphatidylethanolamine [PE(12:0)/(12:0)] and DPPC underwent lateral phase segregation between the gel phase and the fully-interdigitated phase with the addition of ethanol [25]. Similarly, Mason found that there could be phase-separated domains of interdigitated and non-interdigitated gel phases with binary combinations of symmetric and mixed-chain phosphatidylcholines [26].

Therefore, we employed DSC to study the thermodynamic phase behavior of our binary lipid systems. Additionally, we used DPH and β-DPH HPC to determine if the DPPC/F-DPPC and DAPC/F-DPPC mixtures were interdigitated. Fig. 1 shows the chemical structures of the lipids and fluorescent probes used in these experiments. A decrease in intensity has been used successfully as an indicator of the interdigitated phase [27,28]. This change was attributed to quenching caused by increased exposure to the aqueous solvent that occurs with interdigitation (see Fig. 2). For comparison, we also measured the fluorescence intensity of ethanol-induced interdigitated DPPC versus the intensity of F-DPPC with and without ethanol.

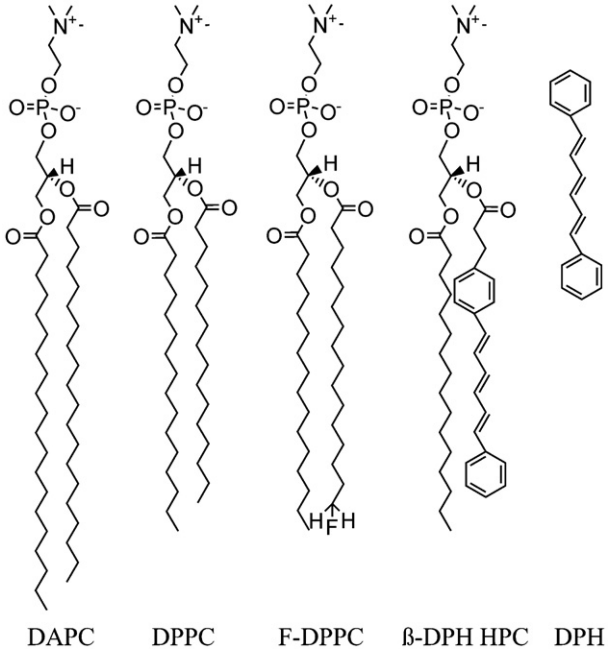

Fig. 1. The chemical structures of the lipids and probes used in this study.

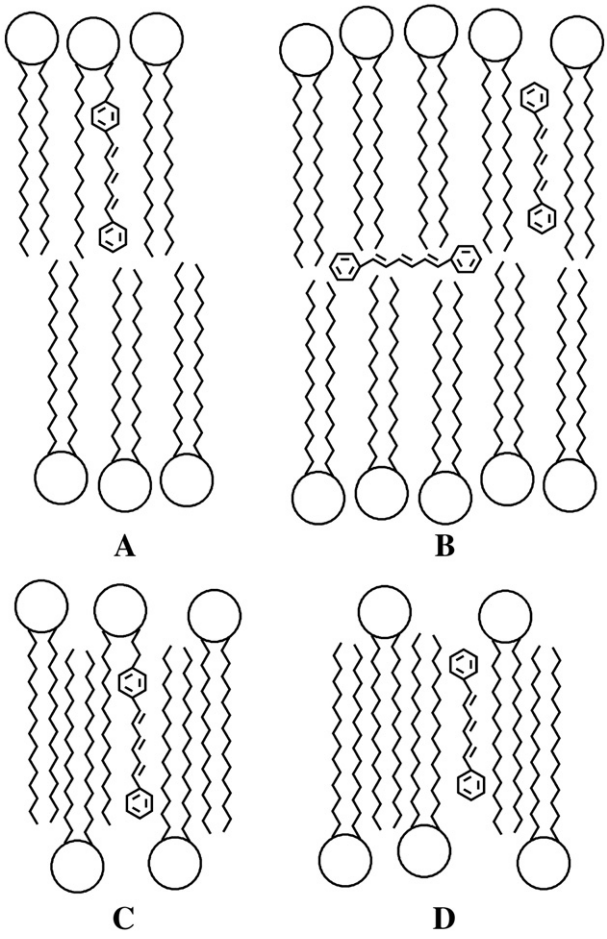

Fig. 2. Representation of the locations of β-DPH HPC and DPH in non-interdigated and interdigitated membranes: (A) β-DPH HPC in a non-interdigitated bilayer; (B) Two possible locations of DPH in a non-interdigitated bilayer; (C) β-DPH HPC in an interdigitated system; (D) DPH in an interdigitated system.

2. Materials and methods

2.1. Materials

The sixteen carbon-chain phosphatidylcholine 1,2-dipalmitoyl-*sn*-glycero-3-phosphocholine (DPPC), the twenty carbon-chain phosphatidylcholine, 1,2-diarachidoyl-*sn*-glycero-3-phosphocholine (DAPC), and the fluorinated 1-palmitoyl-2-(16-fluoropalmitoyl)-sn-glycero-3-phosphocholine (F-DPPC) were purchased from Avanti Polar Lipids (Alabaster, AL). All water used was purified and double-deionized by a Milli-Q filtration system. Chloroform (99.9% assay) stabilized with ~0.75% ethanol was purchased from Fisher Scientific (Pittsburg, PA). The fluorescent probes, 1,6-diphenyl-1,3,5-hexatriene (DPH) and 2-(3-(diphenylhexatrienyl) propanoyl)-1-hexadecanoyl-sn-glycero-3-phosphocholine (β-DPH HPC), were obtained from Molecular Probes (Eugene, OR). Methanol (≥99.9% assay) was purchased from Sigma-Aldrich (St. Louis, MO). Dehydrated 200-proof ethanol was purchased from Quantum Chemical Corporation (New York, NY). All chemicals were used without further purification.

2.2. Differential scanning calorimetry

For the DSC and fluorescence studies, stock solutions of F-DPPC, DPPC, and DAPC were prepared in chloroform and combined to create

the correct molar ratio. Each sample was evaporated to dryness in a fume hood and under high vacuum for at least 10 h to remove any residual solvent. These samples were later hydrated and incubated at 60 °C for an hour with periodic vortexing to form multilayers. All calorimetry samples contained 3 mg lipid and were hydrated with 150 µl of water. These were analyzed with a Calorimetry Sciences Corporation multi-cell DSC-HT Model 4100 DSC. A sequence of heating and cooling scans were recorded from 40 °C to 70 °C for DAPC/F-DPPC and 25 °C to 55 °C for DPPC/F-DPPC at a rate of 10 °C/h. Enthalpy measurements were calculated from the calorimetry data using the integration function on OriginPro 7.5.

2.3. Fluorescence spectroscopy

The fluorescence samples were prepared as above, but instead contained 3 ml of solution with a lipid concentration of 0.64 mg/ml to minimize light scattering. Some samples were prepared with 100 mg/ml ethanol in water, since DPPC interdigitates at concentrations above ~50 mg/ml ethanol [29]. Besides these exceptions, 100% deionized water was used. The fluorescent probes (β-DPH HPC and DPH) were prepared in methanol and added to the lipid solution in chloroform so that the lipid-to-probe mole ratio was 500:1. The solutions were thoroughly mixed to ensure consistency.

All samples were placed in a quartz cuvette with a magnetic stirring bar. To prevent oxygen quenching, the solutions were bubbled with nitrogen for 10 min. The fluorescence measurements were carried out using an ISS K2 Multi-Frequency Cross-Correlation Phase and Modulation Fluorometer with a Xenon Arc Lamp operating at 15 A. Excitation was carried out at 360 nm and the emission was measured at 430 nm. A steady flow of nitrogen was passed through the sample compartment to prevent oxidation. In order to maintain a constant sample temperature, a Neslab RTE-111 circulating bath was set at 30 °C for all measurements.

3. Results

3.1. DSC: DPPC/F-DPPC

Fig. 3 shows the T_m as determined by DSC for different mixtures of DPPC and F-DPPC. This represents either the transition from ripple gel (P'_β) to the liquid crystalline (L_α) phase or from the interdigitated ($L_\beta I$) phase to the L_α phase. Both the heating and cooling transition temperatures are shown. Shoulder peaks were seen only in the 30–50 mol% F-DPPC range. Our DSC results reveal that the thermodynamic properties from 0 to 40 mol% versus from 40 to 100 mol% F-DPPC were dramatically different in three respects: variations in the T_m, the shape of the T_m peak, and the hysteresis between heating and cooling transitions.

In the heating transitions, there are two different rates at which the T_m increased with additional F-DPPC (see dashed lines in Fig. 3). From 0 to 40 mol% F-DPPC, it increased at an average of only 0.03 °C/% F-DPPC. In fact, at 10% F-DPPC, the T_m was lower than that of the pure DPPC. The rate increased almost four-fold to 0.11 °C from 40 to 100 mol% F-DPPC. This increase in T_m is present, but less pronounced, in the cooling scans where the corresponding rates were 0.03 °C versus 0.06 °C.

For the low mol% F-DPPC mixtures, some of these peaks were sharper and taller than the pure DPPC peak. However, the T_m peak became broader as the ratio of F-DPPC increased. The heating peaks also became more broad and asymmetrical than their corresponding peaks in the cooling scans (especially in the 40–70 mol% F-DPPC range), suggesting that the heating and cooling transitions had different kinetics (see Fig. 4).

The hysteresis in the T_m further supports that F-DPPC has two different effects (see Fig. 5). Below ~40 mol% F-DPPC, the hysteresis was slightly lower than that observed in pure DPPC. However, above 40 mol% F-DPPC, there was an approximately threefold increase in the hysteresis.

3.2. DSC: DAPC/F-DPPC

In contrast, our calorimetry data for the DAPC/F-DPPC system indicate that these lipids were much less miscible than DPPC/F-DPPC. This is evident from the heating and cooling main transition temperatures from our mixtures of DAPC and F-DPPC (see Fig. 6). From ~20 to 35 mol% F-DPPC, there are two T_m peaks: one close to the T_m temperature of DAPC and one close to that of F-DPPC. Unlike the DPPC/F-DPPC system, there is no steady change in the T_m as the mol% of F-DPPC increases. Instead, the bulk of the peaks appeared near the T_m of either DAPC or F-DPPC, with only a limited amount of transitions

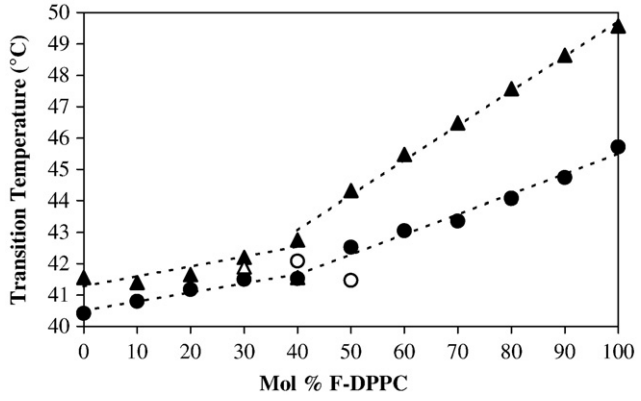

Fig. 3. The main transition temperature (T_m) of DPPC/F-DPPC mixtures determined by DSC. Heating scans shown by filled triangles (▲). Cooling scans shown by filled circles (●). Shoulder peaks indicated by unfilled triangles for heating scans (△) and circles for cooling scans (○). Slopes for 0–40 and 40–100 mol% F-DPPC are shown as dotted lines.

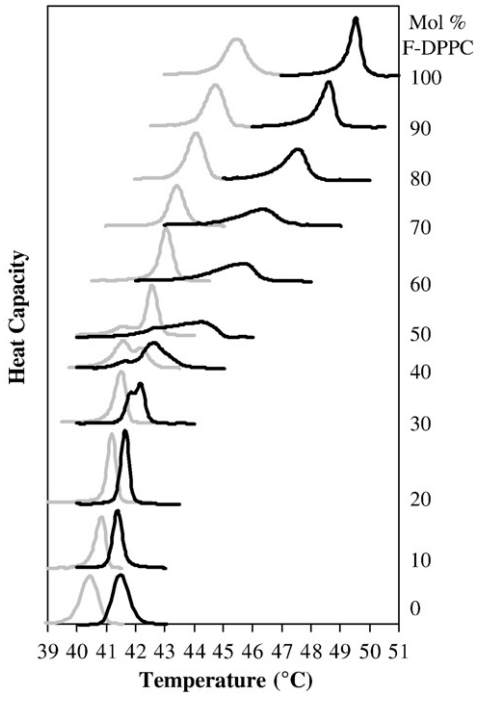

Fig. 4. Heating (black lines) and cooling (gray lines) DSC thermograms of the T_m of the DPPC/F-DPPC system are shown. The cooling scans have been inverted to allow comparison with the heating thermograms. The mol% F-DPPC is labeled next to each mixture. For clarity, the thermograms are also offset vertically.

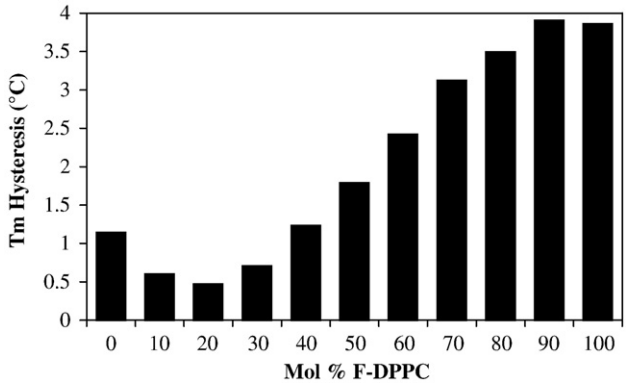

Fig. 5. Hysteresis (or difference in T_m temperature between heating and cooling scans) determined by DSC for the DPPC/F-DPPC system.

in between. This can be seen in the heating and cooling thermograms shown in Fig. 7. Sizable shoulder peaks appeared in the cooling scans at 10, 70, and 80 mol%, and on the heating scans at 25 mol% F-DPPC.

When the ratio of F-DPPC increased, the large sharp peak close to the T_m of DAPC grew smaller and broader. The position of this higher temperature peak did not shift dramatically in temperature with the addition of more F-DPPC as in the DPPC/F-DPPC system. A slight decrease in T_m was observed from 0 to 35% F-DPPC, but only ~1.6 °C versus the T_m of DAPC. The lower temperature peak also revealed a small temperature depression versus the T_m of F-DPPC (20–100 mol% F-DPPC). These separate, lower peaks emerged a little below the T_m of pure F-DPPC (a decrease of ~1.9 °C).

Another difference between the DSC data obtained from DAPC/F-DPPC versus DPPC/F-DPPC was the lack of an elevated hysteresis (see Fig. 8). This was the case for both the lower and higher temperature T_m peaks. Even when two T_m peaks coexisted (20–35 mol% F-DPPC), the hysteresis remained small for both transitions. Only at around 90 mol% F-DPPC did the hysteresis become larger than that of pure DAPC, although the shoulder peaks on the cooling scans at 70 and 80 mol% F-DPPC foreshadowed this behavior.

3.3. β-DPH HPC and DPH fluorescence

Fig. 9 demonstrates the percent change in intensity of β-DPH HPC and DPH in DPPC/F-DPPC relative to pure DPPC in water. As in the DSC data, there are two ratio-dependent effects of F-DPPC. The intensity of

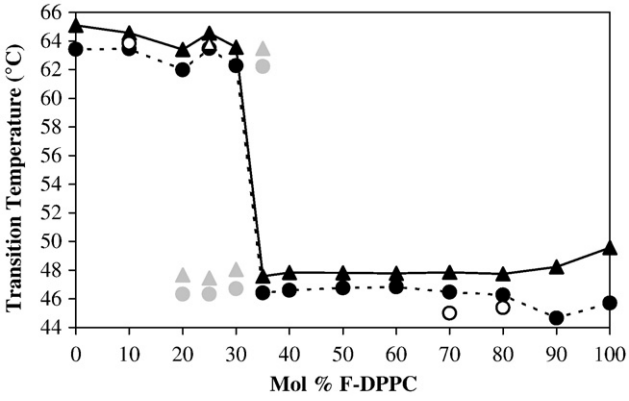

Fig. 6. Main transition temperature (T_m) of DAPC/F-DPPC mixtures determined by DSC. Heating scans shown by filled triangle with solid connecting line (▲). Cooling scans shown by filled circle connected by dotted line (●). Smaller, secondary T_m peaks are indicated by gray triangles (▲) for heating scans and gray circles (●) for cooling scans. Shoulder peaks indicated by unfilled triangles for heating scans (Δ) and unfilled circles for cooling scans (○).

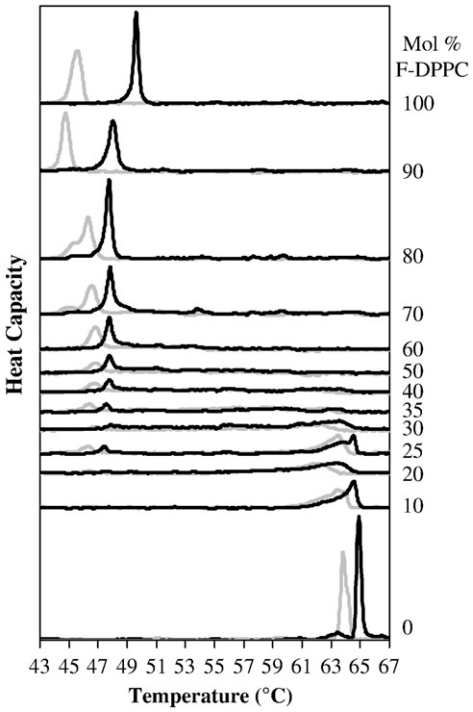

Fig. 7. The DAPC/F-DPPC heating (black lines) and cooling (gray lines) thermograms are shown. The cooling scans have been inverted to allow comparison with the heating thermograms. Since there are multiple peaks in the DAPC/F-DPPC system, the entire baseline is shown. The mol% F-DPPC is labeled next to each mixture. For clarity, the thermograms are also offset vertically.

free DPH greatly declined from 0 to 60 mol% and increased from 60 to 100 mol% F-DPPC. From ~40 to 90 mol%, the decrease was greater than in pure F-DPPC, where the intensity decreased 30%. β-DPH HPC showed little change in intensity from 10 to 30 mol% F-DPPC, but above 30% the intensity gradually decreased with more F-DPPC. Similar to free DPH, the intensity decreased 26% in pure F-DPPC.

In addition, the intensity changes of DPH and β-DPH HPC in DPPC and F-DPPC samples with 100 mg/ml ethanol are shown in Fig. 10. As was reported by Nambi et al., there is a large difference between DPH and β-DPH HPC in DPPC when ethanol is introduced [28]. However, the probes had a similar decrease in the F-DPPC samples. Adding ethanol to F-DPPC caused the fluorescence intensity of both probes to increase slightly.

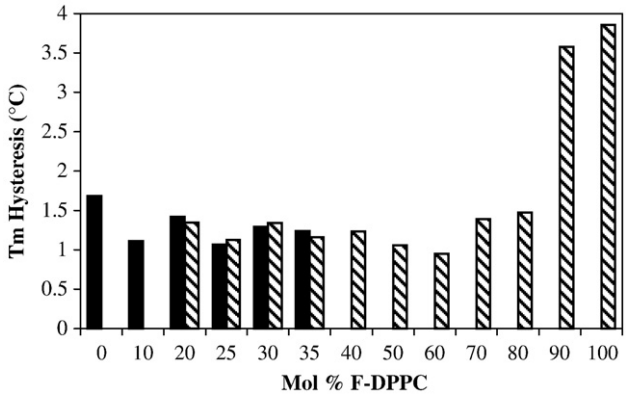

Fig. 8. Hysteresis (or difference in T_m temperature between heating and cooling scans) determined by DSC for the DAPC/F-DPPC system. The thermodynamic peaks occurring at higher temperatures are shown by the black bars and the peaks appearing at lower temperatures are shown by dashed black and white bars. From 20 to 35 mol% F-DPPC, there are two coexisting main transition peaks.

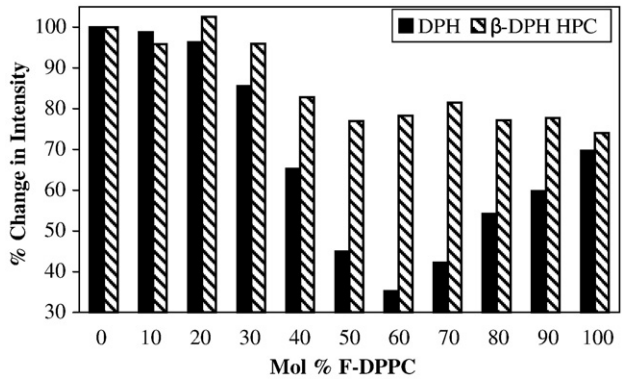

Fig. 9. Fluorescence intensity of DPH and β-DPH HPC in the F-DPPC/DPPC system. Results are shown as a percentage of change versus pure DPPC in water. DPH is shown by solid black bars. β-DPH HPC is shown by black and white dashed bars.

We were unable to obtain reliable fluorescence results with the DAPC/F-DPPC system for two reasons. First, there was excessive foaming of the sample during the preparation process. Steps such as varying incubation temperature, increasing stirring, or allowing the samples to remain undisturbed were ineffective at removing the foam. As a result, the intensity readings were far below that of the equivalent mixtures of DPPC/F-DPPC. Second, the lipid mixture did not form a homogenous solution, as the lipid system tended to aggregate together in clumps. More vigorous vortexing, increased incubation temperature, and sonication improved the mixing only temporarily. This behavior is most likely due to the longer acyl chain lengths on DAPC and the resulting increase in hydrophobicity.

3.4. Main transition enthalpy and disappearance of the pretransition

The enthalpy values for pure samples of F-DPPC, DPPC, and DAPC (~10.6, 8.0, and 13.6 kcal/mol) were close to previously reported values of ~9.8, 8.2, and 13.3 kcal/mol respectively [8,30]. Total enthalpy values were used for the mixed systems because there was the possibility of phase segregation and the existence of multiple peaks. In addition, the results are qualitative as the enthalpy values obtained in both mixed systems had a large margin of error. The enthalpy of the main transition in the DPPC/F-DPPC system gradually increased (towards the enthalpy of F-DPPC) as the mol% of F-DPPC increased. In contrast, there was a sharp drop of ~60% at 10 mol% F-DPPC in the DAPC/F-DPPC system. From 20 to 90 mol% F-DPPC, the DAPC/F-DPPC enthalpy values averaged around 10 kcal/mol, but revealed no particular trend.

There was no detectable pretransition from the planar gel phase (L'_β) to the rippled gel phase (P'_β) in either of the mixed systems.

4. Discussion

4.1. Miscibility, phase separation, and domain formation

Previous studies have extensively established that mixed lipid systems have the potential to separate into domains [19–26]. The most likely causes for domain formation with DPPC/F-DPPC and DAPC/F-DPPC are thermodynamic phase segregation and hydrophobic mismatch. Overall, the heating and cooling DSC thermograms reveal that DPPC and F-DPPC are largely miscible (Fig. 4). As a result, the DPPC/F-DPPC phase transition behavior was a composite of the individual lipids. Because there is only one T_m thermodynamic peak, it is highly probable that the interdigitated lipid domains caused by F-DPPC coexist in the same membrane with non-interdigitated lipids. We derived a phase diagram from the onset and completion temperatures of the DPPC/F-DPPC T_m peaks to show the probable areas for the presence of multiple phases (see Fig. 11). Estimations for the presence of interdigitated gel ($L_\beta I$), non-interdigitated planar gel (L'_β), and liquid crystalline (L_α) phase lipids are labeled. This diagram demonstrates that the mixture exhibits continuous miscibility.

In contrast, our DSC results for the DAPC/F-DPPC system support that these lipids are less miscible. Although the T_m of DPPC and DAPC are not drastically different from that of F-DPPC (−9 °C and +16 °C respectively), DPPC exhibits far more ideal mixing behavior with F-DPPC. Therefore, the difference in chain length may be the most important factor contributing to miscibility, since while F-DPPC and DPPC both have 16-carbon acyl chains, DAPC is longer by 4 acyl carbon atoms. As a result, the DAPC/F-DPPC membranes are likely to be asymmetrical and irregularly organized.

For comparison, the phase diagram for DAPC/F-DPPC is shown in Fig. 12. It can be seen that the DAPC/F-DPPC mixtures are less ideal than DAPC/DPPC [31]. Since the only difference between DPPC and F-DPPC is the addition of the fluorine atom, the decrease in miscibility must be due to this chemical substitution. It is unlikely that F-DPPC and DAPC were completely separated out into different membranes or domains. The most reasonable explanation of the mixing behavior of DAPC/F-DPPC is that the lipids segregate into DAPC-rich and F-DPPC-rich regions. According to the DSC hysteresis results, these F-DPPC-rich domains may be in the planar gel phase (L'_β) rather than the $L_\beta I$ phase below the T_m except at very high mol% of F-DPPC (Fig. 8). For example, the hysteresis of the F-DPPC-rich portions did not increase due to interdigitation even when two T_m peaks were present (Fig. 8). These lower temperature transitions had a similar degree of hysteresis

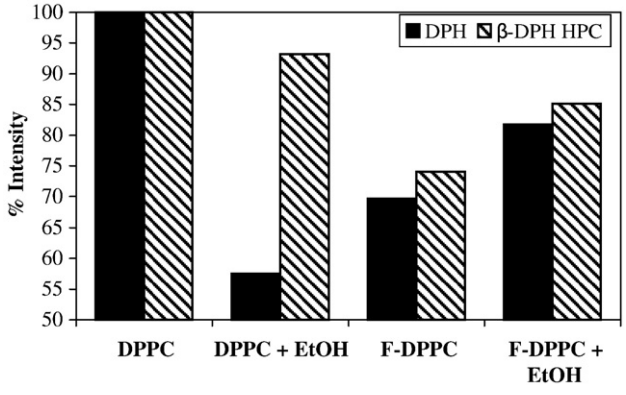

Fig. 10. Fluorescence intensity of DPH and β-DPH HPC in DPPC and F-DPPC with and without 100 mg/ml EtOH. Bars demonstrate intensity as a percentage relative to DPPC in water (shown by the leftmost bar). DPH is shown by solid black bars. β-DPH HPC is shown by black and white dashed bars.

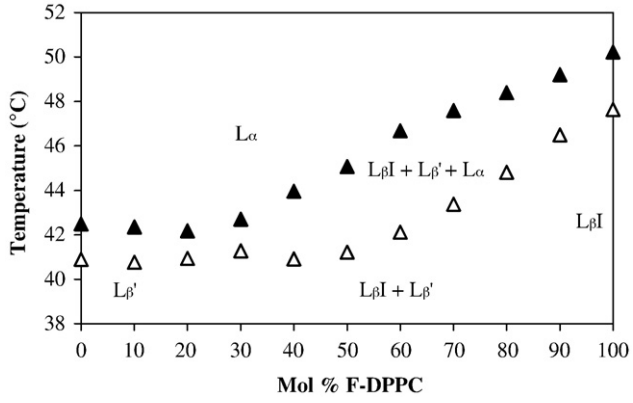

Fig. 11. Phase diagram of the DPPC/F-DPPC system. The onset temperatures of the T_m peaks are shown by black triangles (▲) and the completion temperatures by unfilled triangles (△). The approximate regions of the interdigitated gel ($L_\beta I$), planar gel (L'_β), and liquid crystalline (L_α) phases are labeled.

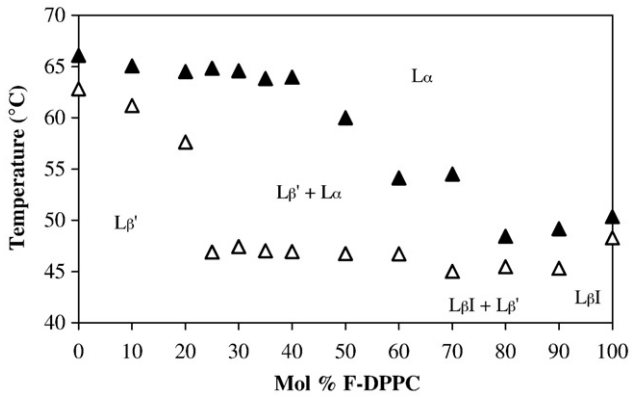

Fig. 12. Phase diagram of the DAPC/F-DPPC system. The onset temperatures of the T_m peaks are shown by black triangles (▲) and the completion temperatures by unfilled triangles (△). The approximate regions of the interdigitated gel ($L_\beta I$), planar gel (L'_β), and liquid crystalline (L_α) phases are labeled.

compared to the higher temperature peaks at the same mol% of F-DPPC. This could mean that DAPC has a disrupting effect on the formation of the $L_\beta I$ phase by F-DPPC. If this is the case, then F-DPPC-rich domains can only incorporate a small amount of DAPC before the $L_\beta I$ phase becomes unfavorable.

4.2. Effect of nucleation sites, lipid packing, and interfacial regions

The main transitions of saturated phosphatidylcholines are highly cooperative. As a result, the transition widths can be narrower than 0.1 °C and are close to an ideal first order transition [30]. This cooperativity depends on the interfacial free energy of clusters of coexisting phases at the transition temperature [32–34]. Moreover, the activation energy for the nucleation of these domains is heavily dependent on temperature [35]. As a consequence, there are kinetic barriers to phase transitions that depend on the nucleation rate of the new phase. Nucleation sites can therefore explain, for some of the DPPC/F-DPPC and DAPC/F-DPPC mixtures, why the T_m drops, why the T_m peaks are sharper, and why the hysteresis is reduced.

For instance, in the DAPC/F-DPPC mixtures, the T_m peaks are below the respective T_m temperature of DAPC and F-DPPC. In addition, the T_m temperature of DPPC/F-DPPC drops slightly at low amounts of F-DPPC. Some of these transitions also have T_m peaks that are narrow in shape. The combination of a T_m temperature reduction and a decrease in the transition width is an unusual one. Most commonly, with the introduction of compounds that decrease the T_m (such as anesthetics and cholesterol) the transition peaks also broaden, as would be expected with the introduction of impurities [36–38]. Furthermore, with most lipid mixtures, the transition peak broadens rather than sharpens [18,22,25,26].

There are two possible explanations for the T_m behavior in these mixtures of DPPC/F-DPPC and DAPC/F-DPPC. First, the small decrease in the T_m could result from one of the lipids acting as an impurity, lowering the phase transition akin to the melting-point depression of a solid. Second, the mixing could create local disturbances that act as nucleation sites. These may account for the increased cooperativity and perhaps a lower thermal energy requirement for the transition.

The reduction in hysteresis of the T_m may also be explained in terms of lipid organization and nucleation. For most of the DAPC/F-DPPC system, the hysteresis of the T_m is less than that of DAPC. There is also a decrease in hysteresis in some of the DPPC/F-DPPC mixtures. This may be due to the fact that both nucleation sites and interfaces between gel phase domains have the potential to alter the reversibility of the T_m [39].

Furthermore, the decrease in enthalpy in the DAPC/F-DPPC system may be related to uneven mixing and the resulting interfacial regions. The decrease is best attributed to the loss of Van der Waals interactions between the long acyl chains of DAPC. After all, these forces greatly contribute to the chain length-dependent high T_m enthalpy of DAPC [33]. This decrease also reinforces the idea that DAPC and F-DPPC interact in some capacity, even if it is only to upset the normal organization of the pure lipids.

Lastly, our data support that disordered lipid packing has an effect on the fluorescence intensity of DPH and β-DPH HPC. For instance, such disruptions can explain why the fluorescence intensity of free DPH in DPPC/F-DPPC at high amounts of F-DPPC (~40–90 mol%) is lower than the fully-interdigitated 100% F-DPPC (Fig. 9). This agrees with the hypothesis by Rowe that hybrid interdigitated and non-interdigitated membranes should have distinctive properties [25]. It is likely that the membrane thickness would be inconsistent and that there would be unusual interfacial regions between the domains of the different phases. The perturbation caused by these phase boundaries could alter the packing of the lipids, thereby further exposing the probes to the aqueous environment.

4.3. Evidence for the interdigitated phase

Although DSC can only indirectly detect the presence of the $L_\beta I$ phase, previous studies have described key characteristics of the phase. For example, the $L_\beta I$ phase is indicated by the lack of a pretransition and the presence of a large hysteresis between DSC heating and cooling scans [27,29,40–42]. The pretransition is not seen with F-DPPC and other interdigitating lipids because they transition from the planar gel phase (L'_β) to the $L_\beta I$ phase. The irreversibility of the $L_\beta I$ to L_α phase transition is known to result in the hysteresis.

Both of these characteristics are present in our DSC data. However, in some mixed lipid systems there is no pretransition regardless if the membrane is interdigitated or not [25]. This may explain why there is no pretransition peak in any of our DPPC/F-DPPC or DAPC/F-DPPC mixtures. In addition, the initial drop in hysteresis may be due to the nucleation-type effect, but as the F-DPPC ratio increases, the overall hysteresis increases due to the growth of interdigitated F-DPPC-rich domains.

Direct evidence of interdigitation can be obtained from the fluorescence intensity depression of both probes embedded in the lipids. In the $L_\beta I$ phase, the width of the bilayer decreases, the midplane of the bilayer disappears, and there is greater headgroup separation [1,28]. These changes expose more of the lipid acyl chains and the hydrophobic DPH probes to the surrounding aqueous solvent (see Fig. 2). The sensitivity of the DPH moiety to this environmental change is the basis for the detection of interdigitation. Therefore, the decreases in intensity of DPH and β-DPH HPC support the conclusion by Hirsh et al. that F-DPPC interdigitates in the gel phase [8].

4.4. Fluorophore behavior

β-DPH HPC has photophysical characteristics similar to very free DPH, as the emission spectrum at 25 °C is nearly identical to DPH [43]. Therefore, the discrepancies between DPH and β-DPH HPC are most likely a result of their molecular structures, not because of different fluorescent properties. DPH is very hydrophobic, has a long molecular structure of ~14 Å, and a rigid rodlike shape which makes it able to pack in tightly with the acyl chains [44]. However, with β-DPH HPC, the DPH moiety is chemically attached to a lipid structure. The resulting depth of the DPH moiety in non-interdigitated membranes may be a factor, as free DPH is located slightly closer to the membrane surface relative to β-DPH HPC [44]. Partitioning is also important because the immediate probe environment is the most significant factor affecting fluorescence intensity. While we do not know the extent to which DPH and β-DPH HPC are segregated in the DPPC/F-DPPC and DAPC/F-DPPC systems, phospholipid-bound DPH derivatives are generally more prone to partitioning into domains while

DPH is homogeneously distributed [43,45–47]. Most importantly, the intensity of free DPH and β-DPH HPC always decreases in the $L_{\beta}I$ phase.

While there is broad agreement that the DPH moiety of β-DPH HPC is restricted to locating parallel to the acyl chains of the lipids [28,44,48,49], there are two possible orientations for free DPH in non-interdigitated bilayers. How favored each position is over the other is a matter of some dispute. Nambi et al. hypothesized that the larger intensity depression of free DPH versus β-DPH HPC may be due to the fact that the orientation with DPH in the midplane of the membrane and perpendicular to the hydrocarbon chains becomes untenable in an interdigitated system [28]. In agreement with this interpretation, Kao et al. concluded that DPH relocates in a similar fashion in mixed-interdigitated bilayers formed by lipids with asymmetrical acyl chains [50]. However, Kaiser and London argue that DPH primarily orients parallel to the hydrocarbon chains in non-interdigitated bilayers [44]. In this case, the intensity drop in interdigitated membranes is a result of quenching due to exposure resulting from a closer proximity to the aqueous solvent, not from the reorientation of the DPH molecule.

Our F-DPPC results gravitate towards the position of Kaiser and London. The addition of ethanol affects the two probes in DPPC and F-DPPC membranes in a manner that suggests that there is a secondary interaction besides the induction of interdigitation. One possibility is that the ethanol aggregates around the exposed hydrophobic regions of the probes and acts as a shield against the aqueous solution. This could provide a less polar environment, allowing the probes to fluoresce more intensely. As a consequence, in the absence of alcohol, β-DPH HPC may be a more robust indicator of interdigitation than was previously thought.

Acknowledgments

We would like to thank the Fletcher Jones Foundation, the National Science Foundation, and the Howard Hughes Medical Institute. In addition, we would like to acknowledge Dr. Weidong Wang for his invaluable technical advice and assistance.

References

[1] J.L. Slater, C.H. Huang, Interdigitated bilayer membranes, Prog. Lipid Res. 27 (1988) 325–359.
[2] S.A. Simon, T.J. McIntosh, Interdigitated hydrocarbon chain packing causes the biphasic transition behavior in lipid/alcohol suspensions, Biochim. Biophys. Acta 773 (1984) 169–172.
[3] L. Löbbecke, G. Cevc, Effects of short-chain alcohols on the phase behavior of and interdigitation of phosphatidylcholine bilayer membranes, Biochim. Biophys. Acta 1237 (1995) 59–69.
[4] E.S. Rowe, T.A. Cutrera, Differential scanning calorimetric studies of ethanol interactions with distearoylphosphatidylcholine: transition to the interdigitated phase, Biochemistry 29 (1990) 10398–10404.
[5] T. Hata, H. Matsuki, S. Kaneshina, Effect of local anesthetics on the bilayer membrane of dipalmitoylphosphatidylcholine: interdigitation of lipid bilayer and vesicle–micelle transition, Biophys. Chem. 87 (2000) 25–36.
[6] L.F. Braganza, D.L. Worcester, Hydrostatic pressure induces hydrocarbon chain interdigitation in single-component phospholipid bilayers, Biochemistry 25 (1986) 2591–2596.
[7] D. Worchester, B. Hammouda, Interdigitated hydrocarbon chains in C20 and C22 phosphatidylcholines induced by hydrostatic pressure, Phys. B. Condensed Matter 241 (1997) 1175–1177.
[8] D.J. Hirsh, N. Lazaro, L.R. Wright, J.M. Boggs, T.J. McIntosh, J. Schaefer, J. Blazyk, A new monofluorinated phosphatdylcholine forms interdigitated bilayers, Biophys. J. 75 (1996) 1858–1868.
[9] J.R. Silvius, in: P.C. Jost, O.H. Griffith (Eds.), Lipid–Protein Interactions, Thermotropic Phase Transitions of Pure Lipids in Model Membranes and Their Modifications by Membrane Proteins, vol. 2, John Wiley and Sons, New York, 1982, pp. 239–281.
[10] R. Koynova, M. Caffrey, An index of lipid phase diagrams, Chem. Phys. Lipids 115 (2002) 107–219.
[11] C. Santaella, P. Vierling, J.G. Riess, T. Gulik-Krzywicki, A. Gulik, B. Monasse, Polymorphic phase behavior of perfluoroalkylated phosphatidylcholines, Biochim. Biophys. Acta 1190 (1994) 25–39.
[12] C. Santaella, P. Vierling, Molecular order and mobility within liposomal membranes made from highly fluorinated phospholipids, Chem. Phys. Lipids 77 (1995) 173–177.
[13] F. Frézard, C. Santaella, P. Vierling, J.G. Riess, Permeability and stability in buffer and in human serum of fluorinated phospholipid-based liposomes, Biophys. Biochim. Acta 1192 (1994) 61–70.
[14] F. Frézard, C. Santaella, M.J. Montisci, P. Vierling, J.G. Riess, Fluorinated phosphatidylcholine-based liposomes: H^+/Na^+ permeability, active doxorubicin encapsulation and stability in human serum, Biophys. Biochim. Acta 1194 (1994) 61–68.
[15] J.F.M. Post, E.E.J. De Ruiter, H.J.C. Berendsen, A fluorine NMR study of model membranes containing ^{19}F-labeled phospholipids and an intrinsic membrane protein, FEBS Lett. 132 (1981) 257–260.
[16] M.P. Krafft, Fluorocarbons and fluorinated amphiphiles in drug delivery and biomedical research, Adv. Drug Deliv. Rev. 47 (2001) 209–228.
[17] J.P. Rolland, C. Santaella, B. Monasse, P. Vierling, Miscibility of binary mixtures of highly fluorinated double chain glycerophosphocholines and 1,2-dipalmitoylphosphatidylcholine (DPPC), Chem. Phys. Lipids 85 (1997) 135–143.
[18] J.M. Sturtevant, C. Ho, A. Reimann, Thermotropic behavior of some fluorodimystoylphosphatidylcholines, Proc. Natl. Acad. Sci. USA 76 (1979) 2239–2243.
[19] C. Leidy, W.F. Wolkers, K. Jørgensen, O.G. Mouritsen, J.H. Crowe, Lateral organization and domain formation in a two component lipid membrane system, Biophys. J. 80 (2001) 1819–1828.
[20] K. Jørgensen, A. Klinger, R.L. Biltonen, Nonequilibrium lipid domain growth in the gel-fluid two-phase region of a $DC_{16}Pc$-$DC_{22}PC$ lipid mixture investigated by Monte Carlo computer simulation, FT-IR, and fluorescence spectroscopy, J. Phys. Chem. B 104 (2000) 11763–11773.
[21] J.Y.A. Lehtonen, J.M. Holopainen, P.K.J. Kinnunen, Evidence for the formation of microdomains in liquid crystalline large unilamellar vesicles caused by hydrophobic mismatch of the constituent phospholipids, Biophys. J. 70 (1996) 1753–1760.
[22] S. Mabrey, J.M. Sturtevant, Investigation of phase transitions of lipids and lipid mixtures by high sensitivity differential scanning calorimetry, Proc. Natl. Acad. Sci. USA 73 (1976) 3862–3866.
[23] S.L. Veatch, S.L. Keller, Separation of liquid phases in giant vesicles of ternary mixtures of phospholipids and cholesterol, Biophys. J. 85 (2003) 3074–3083.
[24] P. Brûlet, H.M. McConnell, Kinetics of phase equilibrium in a binary mixture of phospholipids, J. Am. Chem. Soc. 98 (1975) 1314–1318.
[25] E.S. Rowe, Induction of lateral phase separations in binary lipid mixtures by alcohol, Biochemistry 26 (1987) 46–51.
[26] J.T. Mason, Mixing behavior of symmetric chain length and mixed chain length phosphatidylcholines in two-component multilamellar bilayers: evidence for gel and liquid-crystalline phase immiscibility, Biochemistry 27 (1988) 4421–4429.
[27] R. Tran, S. Ho, P. Dea, Effects of ethanol on lipid bilayers with and without cholesterol: the distearoylphosphatidylcholine system, Biophys. Chem. 110 (2004) 39–47.
[28] P. Nambi, E.S. Rowe, T.J. McIntosh, Studies of the ethanol-induced interdigitated gel phase in phosphatidylcholines using the fluorophore 1,6-diphenyl-1,3,5-hexatriene, Biochemistry 27 (1988) 9175–9182.
[29] E.S. Rowe, Lipid chain length and temperature dependence of ethanol–phosphatidylcholine interaction, Biochemistry 22 (1983) 3299–3305.
[30] R. Koynova, M. Caffery, Phases and phase transitions of the phosphatidylcholines, Biochim. Biophys. Acta 1376 (1998) 91–145.
[31] C. Gliss, H. Clausen-Schaumann, R. Günther, S. Odenbach, O. Randl, T.M. Bayerl, Direct detection of domains in phospholipid bilayers by grazing incidence diffraction of neutrons and atomic force microscopy, Biophys. J. 74 (1998) 2443–2450.
[32] P. Grabitz, V.P. Ivanova, T. Heimburg, Relaxation kinetics of lipid membranes and its relation to the heat capacity, Biophys. J. 82 (2002) 299–309.
[33] D. Marsh, General features of phospholipid phase transitions, Chem. Phys. Lipids 57 (1991) 109–120.
[34] E. Freire, R. Biltonen, Estimation of molecular averages and equilibrium fluctuations in lipid bilayer systems from the excess heat capacity function, Biochem. Biophys. Acta 514 (1978) 54–68.
[35] D.W. Oxtoby, Nucleation of first-order phase transitions, Acc. Chem. Res. 31 (1998) 91–97.
[36] T.G. Anderson, H.M. McConnell, Condensed complexes and the calorimetry of cholesterol–phospholipid bilayers, Biophys. J. 81 (2001) 2774–2785.
[37] D.B. Mountcastle, R.L. Biltonen, M.J. Halsey, Effect of anesthetics and pressure on the thermotropic behavior of multilamellar dipalmitoylphosphatidylcholine liposomes, Proc. Natl. Acad. Sci. USA 75 (1978) 4906–4910.
[38] H.M. Seeger, M.L. Gudmundsson, T. Heimburg, How anesthetics, neurotransmitters, and antibiotics influence the relaxation processes in lipid membranes, J. Phys. Chem. B. 111 (2007) 13858–13866.
[39] B. Tenchov, On the reversibility of the phase transitions in lipid–water systems, Chem. Phys. Lipids 57 (1991) 165–177.
[40] M.D. Reeves, A.K. Schawel, W. Wang, P. Dea, Effect of butanol isomers on dipalmitoylphosphatidylcholine bilayer membranes, Biophys. Chem. 128 (2007) 13–18.
[41] M.F.N. Rosser, H.M. Lu, P. Dea, Effects of alcohols on lipid bilayers with and without cholesterol: the dipalmitoylphosphatidylcholine system, Biophys. Chem. 81 (1999) 33–44.
[42] J.A. Viero, P. Nambi, L. Herold, E.S. Rowe, Effects of n-alcohols and glycerol on the pretransition of dipalmitoylphosphatidylcholine, Biochim. Biophys. Acta 900 (1987) 230–238.
[43] R.A. Parente, B.R. Lentz, Advantages and limitations of DPHpPC as a fluorescent membrane probe, Biochemistry 24 (1985) 6178–6185.
[44] R.D. Kaiser, E. London, Location of diphenylhexatriene (DPH) and its derivatives within membranes: comparison of different fluorescence quenching analyses of membrane depth, Biochemistry 37 (1998) 8180–8190.

[45] T. Nyholm, M. Nylund, A. Söderholm, J.P. Slotte, Properties of palmitoyl phosphatidylcholine, sphingomyelin, and dihydrosphingomyelin bilayer membranes as reported by different reporter molecules, Biophys. J. 84 (2003) 987–997.
[46] B.R. Lentz, Y. Barenholz, T.E. Thompson, Fluorescence depolarization studies of phase transitions and fluidity in phospholipid bilayers. 1. Single component phosphatidylcholine liposomes, Biochemistry 15 (1976) 4521–4528.
[47] M.P. Andrich, J.M. Vanderkooi, Temperature dependence of 1,6-diphenyl-1,3,5 hexatriene fluorescence in phophoslipid artificial membranes, Biochemistry 15 (1976) 1257–1261.
[48] R.A. Parente, B.R. Lentz, Fusion and phase separation monitored by lifetime changes of a fluorescent phospholipid probe, Biochemistry 25 (1986) 1021–1026.
[49] H. Saito, T. Minamida, I. Arimoto, T. Handa, K. Miyajima, Physical states of surface and core lipids in lipid emulsion and apolipoprotein binding and the emulsion surface, J. Bio. Chem. 271 (1996) 15515–15520.
[50] Y.L. Kao, P.L. Chong, C. Huang, Dynamic motions of 1,6-diphenyl-1,3,5-hexatriene in interdigitated C(18):C(10)phosphatidylcholine bilayers, Biophys. J. 58 (1990) 947–956.